Simulation of conductance and current-induced fluorescence of conjugated chromophores

ARTICLE *in* CHEMICAL PHYSICS LETTERS · DECEMBER 2007

Impact Factor: 1.9 · DOI: 10.1016/j.cplett.2007.10.078

Available online at www.sciencedirect.com
ScienceDirect
Chemical Physics Letters 450 (2007) 144–150
CHEMICAL PHYSICS LETTERS
www.elsevier.com/locate/cplett

Simulation of conductance and current-induced fluorescence of conjugated chromophores

J.B. Maddox [a], U. Harbola [a], G.C. Bazan [b], S. Mukamel [a,*]

[a] Department of Chemistry, University of California, Irvine, CA 92697-2025, United States
[b] Department of Chemistry and Biochemistry, University of California, Santa Barbara, CA 93106-9510, United States

Received 15 September 2007; in final form 24 October 2007
Available online 26 November 2007

Abstract

The conductance and current-induced fluorescence of a single distyryl-benzene and a single distyryl-paracyclophane molecule in a tunneling junction is simulated. Our approach is formulated in terms of the electronic states of the neutral and charged molecular bridge and is applied to calculate the effective tunneling rates. We find that an orbital picture is adequate for describing the conductance of distyryl-benzene; however, a many-electron picture is needed for the paracyclophane linked complex. A strategy for maximizing electroluminescence by controlling the voltage drop across the junction through chemical modification of the molecular bridge is suggested.

1. Introduction

Chromophores derived from paraphenylene–vinylene oligomers are frequently used as model systems to represent individual components of semi-conducting organic materials [1]. A related class of compounds consisting of paracyclophane linked stilbenoids offer additional insight as a well-defined structural model mimicking the crossing of two such molecular wires [2]. It has been demonstrated that donor/acceptor substituents in combination with solvation effects can been used to examine and control the optical response of paracyclophane-based chromophores [3–6]. This high sensitivity of the excited state to solvent/substituent effects makes the paracyclophane structural motif particularly suitable for the design of tailored chromophores for use in biosensing applications [7]. Furthermore, relaxation processes involving torsional rotation about vinylic single bonds [8] can lead to localization of the excited state on the ultra-fast timescale [9,10]. Such considerations may be highly relevant for the design of a molecular based switching devices [11]. Seferos et al., have recently compared the conductance of thiolated self-assembled monolayers of distyryl-benzene and a paracyclophane cross-linked stilbene dimer on gold electrodes [12,13].

In this Letter, we discuss factors to consider in the design of electroluminescent devices based on single molecule components consisting of the molecules 3R and 2Rd, see insets of Fig. 1. We review formulas for calculating the conductance (dI/dV) and current-induced fluorescence (CIF) spectra of a single molecule tunneling junction in terms of the many-electron states of the molecular bridge with N and $N \pm 1$ electrons. Our calculations account for the fact that electron/hole injection and electronic transitions are many-electron processes involving contributions from more than one molecular orbital. We calculate the contributions of different orbitals to the effective tunneling rates through the junction and identify how charge state transitions contribute to the conductance and the optical response of a molecule. Our analysis suggests a possible strategy for maximizing electroluminescence yield through chemical modification of the molecular bridge.

2. Methodology

We consider a tunneling junction consisting of a molecular bridge weakly coupled to two (left and right) metallic

* Corresponding author.
E-mail address: smukamel@uci.edu (S. Mukamel).

0009-2614/$ - see front matter © 2007 Elsevier B.V. All rights reserved.
doi:10.1016/j.cplett.2007.10.078

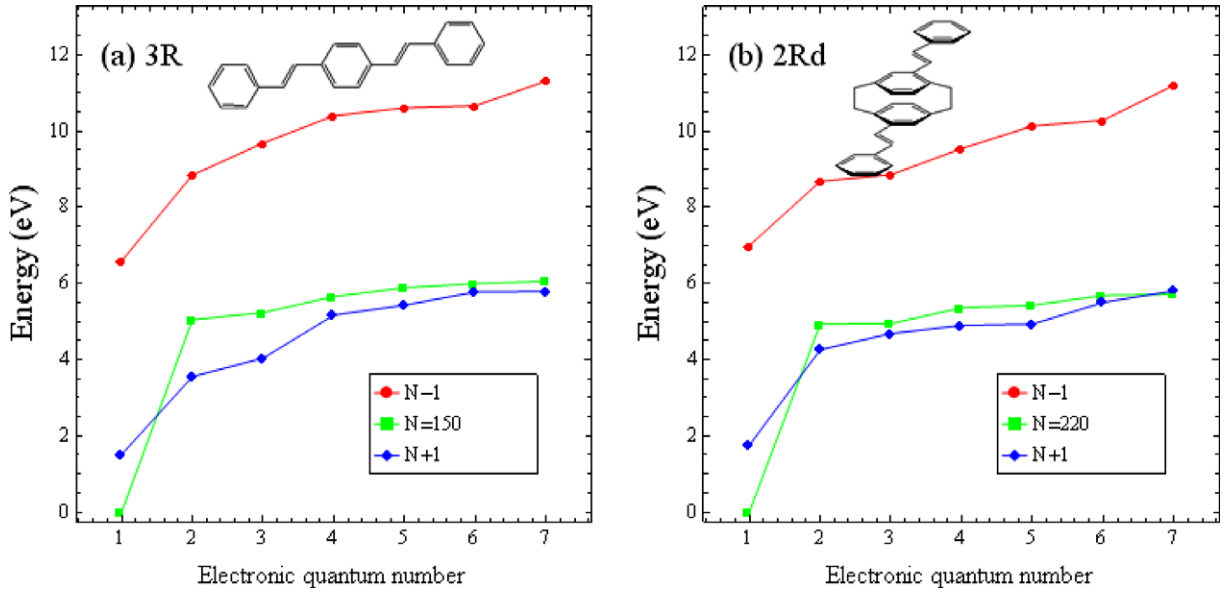

Fig. 1. Electronic energies for the cationic $N-1$ (red circles), neutral N (green squares), and anionic $N+1$ (blue diamonds) of the molecules (a) 3R and (b) 2Rd. N is the number of electrons in the neutral molecule. (For interpretation of the references to colour in this figure legend, the reader is referred to the web version of this article.)

leads. The typical theoretical approach for such systems utilizes self-consistent methods for incorporating the molecule–leads electronic interaction as per the nonequilibrium Greens function theory (NEGFT) of electron transport [14]. Though this approach has proven extremely versitile for describing many different aspects of conductance through molecular–scale junctions [15] its utility for the weak coupling (Coulomb Blockade) regime has recently been questioned [16]. For systems, where the charging energy of the bridge is large one would expect that charge state transition involving excited electronic states may play a more significant role in the conductance.

To examine this in more detail we take the zeroth order solution of the NEFGT and recast the lesser and greater Greens functions in terms of the unperturbed molecular electronic states [17,18]. The resulting perturbative expression for the conductance is second order in the molecule–lead coupling and given by

$$\frac{\mathrm{d}I}{\mathrm{d}V}=\frac{2e}{\hbar}\sum_{X=L,R}\left(\sum_{b\in N+1}\frac{\mu'_X|W^X_{ab}|^2\Gamma_{ab}}{(\mu_X-E_{ba})^2+\Gamma^2_{ab}}+\sum_{b'\in N-1}\frac{\mu'_X|W^X_{b'a}|^2\Gamma_{ab'}}{(\mu_X+E_{b'a})^2+\Gamma^2_{ab'}}\right) \tag{1}$$

where the sum over X runs over the left (L) and right (R) leads with chemical potentials, $\mu_L=E_\mathrm{F}+\eta$ eV and $\mu_R=E_\mathrm{F}-(1-\eta)$ eV, respectively. The applied bias energy is eV, E_F is the Fermi energy of the unbiased ($V=0$) junction, and η is the voltage division factor characterizing an idealized linear potential drop [19]. The index a designates the neutral charge state with N electrons and the b and b' sums run over the many-electron (ground and excited) states of the anion ($N+1$ electrons) and cation ($N-1$ electrons), respectively. $E_{vv'}=E_v-E_{v'}$ is the energy difference between two states. The conductance of the molecular junction exhibits peaks when the either the left or right chemical potential is resonant with either E_{ba} or $E_{ab'}$. Peaks from the anionic or cationic states can occur at either positive or negative bias polarity depending on η. The lineshape of the conductance peaks have a simple Lorenztian form, where the phenomenological total dephasing rate Γ_{ab} takes into account interactions which broaden the molecules electronic energy eigenstates e.g., the molecule–lead electronic coupling and possibly electron–phonon interactions.

The tunneling rates are determined by the factors

$$W^X_{ab}=\sum_i W_i(\mu_X)\langle a|c_i|b\rangle \tag{2}$$

$$W^X_{b'a}=\sum_i W_i(\mu_X)\langle a|c^\dagger_i|b'\rangle \tag{3}$$

where $c^\dagger_i$ and c_i are the creation and annihilation operators for an electron in the ith molecular orbital of the bridge [16]. $W_i(\mu_X)$ is the coupling between an electron in the lead with energy μ_X and the ith molecular orbital. More generally, this can be expressed as a tunneling matrix element W_{iv} between vth level of the lead to the ith molecular orbital of the bridge; these can be computed in different ways such as directly from *ab initio* calculations of an extended molecule [20], by Tersoff–Hamann approach [21,22], or by the generalized Mulliken–Hush method [23]. For infinitely large leads the tunneling elements become a continuous function of energy, $W_{iv}\to W_i(\epsilon_v)$. We will neglect this energy dependence over the range of the applied bias energy i.e., we take the wide-band limit for the molecule–lead electronic coupling and also assign a commensurate dephasing rate $\Gamma_{ab}=\Gamma$ for all of the neutral/charged electronic transitions.

We take the coupling W_i^X to be proportional to the overlap of orbital $|i\rangle$ with a spherically symmetric probe orbital $|\mathbf{r}_X\rangle$ centered about the position $\mathbf{r}_X$ corresponding to the end of an atomically sharp point contact between lead X and the molecular bridge. Moreover, it is convenient to assume that these probe orbitals have perfect resolution i.e., $\langle\mathbf{r}|\mathbf{r}_X\rangle \approx \delta(\mathbf{r}-\mathbf{r}_X)$. In this approximation the coupling is simply given by $W_i \propto \langle\mathbf{r}_X|i\rangle = \phi_i(\mathbf{r}_X)$ where $\phi_i(\mathbf{r}_X)$ is the orbital wavefunction evaluated at the probe's position.

At first glance, the combination of the wide-band limit together with perfect spatial resolution appears counterintuitive; on the one hand, the molecular electronic states are broadened due to the coupling with the leads while at the same time the coupling is assumed to be highly localized in space. An idealized point contact molecular junction may be viewed as a defect in an otherwise infinitely long single file row of metal atoms. In the present context, we imagine that the coupling between the molecule and the neighboring metal atoms is very weak; however, the coupling between metal atoms in the semi-infinite wires is very strong. In this sense, the leads density of states projected onto the contact atoms would be energetically broad but at the same time spatially localized [21]. One possible experimental realization of such a junction might be accomplished using a double-tip STM setup [24].

The matrix elements $\langle a|c_i|b\rangle$ and $\langle a|c_i^\dagger|b'\rangle$ represent the overlap of two states with different numbers of electrons. In our simulations we treat the ground electronic states at the unrestricted Hartree–Fock (HF) level [25]. The excited electronic states $b>0$ and $b'>0$ are calculated using the unrestricted configuration interaction with singly excited determinants (CIS) [26]. Let $|A\rangle$, $|B\rangle$, and $|B'\rangle$ denote to the ground state Slater determinants of the N, $N+1$, and $N-1$ electron molecules. For $N+1$ electrons, the excited states are given by $|b\rangle = \sum_{ij} c_{ij}^b |B_i^j\rangle$, where c_{ij}^b is the CIS coefficient for the singly excited Slater determinant $|B_i^j\rangle$. The excited states of the $N-1$ molecule have a similar definition. We introduce the Slater determinants $|A_i\rangle = |c_i A\rangle$ and $|A^i\rangle = |c_i^\dagger A\rangle$ which are constructed from the molecular orbitals of the neutral HF ground state by adding a hole or electron, respectively, in the ith orbital. The many-body overlap factors are then written as

$$\langle a|c_i|b\rangle = \sum_{jk} c_{jk}^b \langle A^i|B_j^k\rangle \tag{4}$$

$$\langle a|c_i^\dagger|b'\rangle = \sum_{jk} c_{jk}^{b'} \langle A_i|B_j^{k'}\rangle \tag{5}$$

The overlap of two Slater determinants $|P\rangle$ and $|Q\rangle$ is given by the determinant of a matrix $\langle P|Q\rangle = \det\{\mathscr{S}\}$ whose elements $\mathscr{S}_{ij} = \langle\phi_i^P|\phi_j^Q\rangle$ are the overlap integrals between occupied orbitals [27,28].

At high bias energies, the chemical potential of the leads may become resonant with or exceed the energy difference between the ground electronic state of the neutral molecule and the anionic (or cationic) excited electronic states. In this case, electrons/hole injection gives rise to an excited anionic/cationic state. Provided that the coupling between the leads and the molecule is sufficiently weak the excited charge state may have time to relax and/or emit a photon before the charge carrier can exit the bridge. This current-induced fluorescence (CIF) is somewhat analogous to the laser induced fluorescence (LIF) in the sense that the applied bias plays the same role as the excitation laser field [18,29]. One important difference is that in CIF the tunneling channel through the charged molecular states remains open once the bias energy exceeds the transition energies E_{ba} or $E_{ab'}$; hence, the emission will increase with the bias and then saturate. However, in LIF the excitation ceases when the (monochromatic) laser field is tuned beyond the width of the optical transition. Thus the derivative of the CIF signal with respect to the bias is more closely related to LIF. The CIF signal is related to the expectation value of the rate of change of the photon number operator N_S taken as the trace over the total density matrix of the junction. The lowest order contribution to the CIF in the molecule–field (in the dipole approximation) and molecule–lead coupling is given by

$$\frac{\mathrm{d}}{\mathrm{d}V}\langle N_S\rangle = \frac{4e^2\epsilon_S^2\Gamma}{\hbar}\left(\frac{\mathrm{d}S_n}{\mathrm{d}V} - \frac{\mathrm{d}S_p}{\mathrm{d}V}\right) \tag{6}$$

where $\epsilon_S \propto \sqrt{\omega_S}$ and

$$\frac{\mathrm{d}S_n}{\mathrm{d}V} = \sum_{X=L,R} \frac{|W_{ab}^X|^2|\mu_{bc}|^2}{(\Gamma^2 + (\hbar\omega_S - E_{bc})^2)(4\Gamma^2 + (\mu_X - \hbar\omega_S - E_{ca})^2)} \tag{7}$$

$$\frac{\mathrm{d}S_p}{\mathrm{d}V} = \sum_{X=L,R} \frac{|W_{b'a}^X|^2|\mu_{b'c'}|^2}{(\Gamma^2 + (\hbar\omega_S - E_{b'c'})^2)(4\Gamma^2 + (\mu_X + \hbar\omega_S + E_{c'a})^2)} \tag{8}$$

are the contributions from transitions involving the negatively and positively charged states, respectively. We include five electronic states: a the neutral ground state, b and b' the anionic and cationic first excited states, respectively, and c and c' the anionic and cationic ground states, respectively. μ_{bc} and $\mu_{b'c'}$ are the electric transition dipole moments and $\hbar\omega_S$ is the observed photon energy. The CIF signal is a two-dimensional spectrum that depends on both the photon and applied bias energies [18].

Before moving on to our results, we note that our expressions for the conductance and CIF do not address the important issue of coupling between the electronic and nuclear degrees of freedom in the junction [30,31]. A more rigorous approach that fits with present formulation of the current in terms of many-electron states might be to recast the molecular Greens functions in terms of vibronic states (electronic + vibrational direct product) such that Eqs. (2) and (3) would include an appropriate set of Franck–Condon factors. This avenue would require the calculation of relaxed nuclear geometries and normal mode analysis for each electronic state involved in the conductance; however, this goes beyond the scope of the present study.

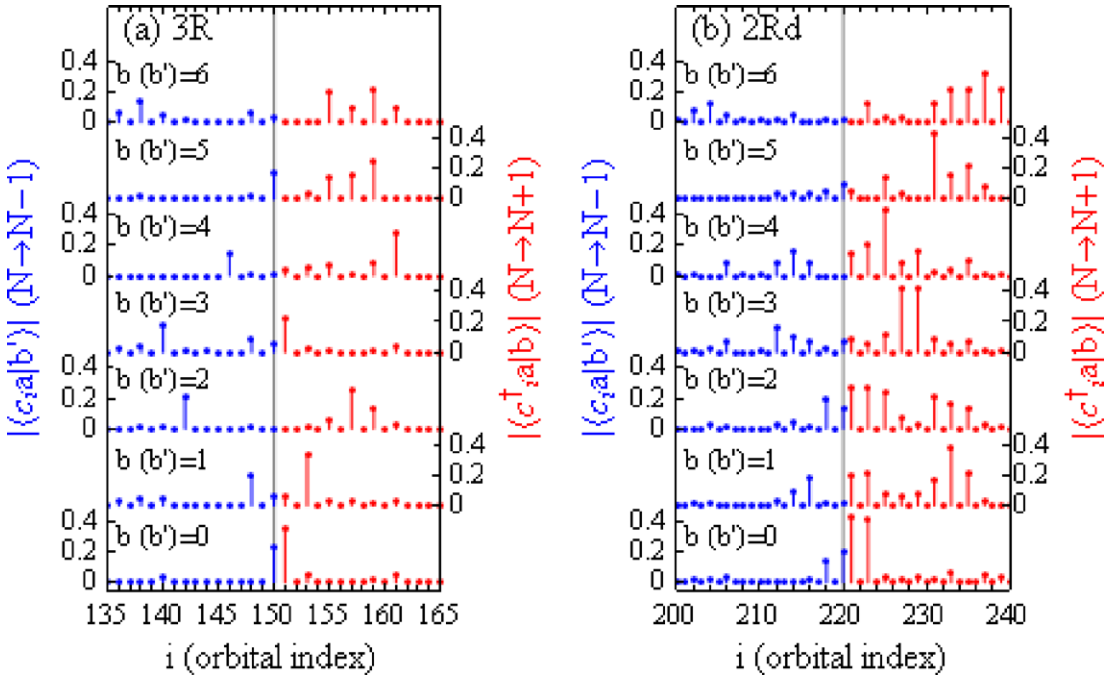

Fig. 2. Many-body overlap factors vs. orbital index for (a) 3R and (b) 2Rd. The gray line designates the highest occupied orbital of the neutral molecule with N electrons.

3. Results and discussion

We have simulated the conductance and CIF of 3R and 2Rd. Our analysis is based on electronic structure calculations at the unrestricted HF and CIS level with a 6-31G basis set [32]. This level of quantum chemistry was chosen more for computational convenience rather than accuracy. In principle, any method from which the many-electron overlap matrix elements, Eqs. (2) and (3), can be derived would also be appropriate.

First, an optimized minimum energy ground state conformation of neutral 3R was found; this geometry was then used to calculate the ground and six excited electronic wavefunctions for the neutral, anionic, and cationic species. A similar set of calculations were made for the 2Rd molecule. Fig. 1a shows the electronic energy levels of neutral and charged 3R as a function of the electronic quantum number. The neutral ground state has the lowest energy and is taken as the reference. The lowest energy electronic transition from the ground state is larger for the neutral molecule compared to the charged species and the cationic states have much higher energies compared with both the neutral and anionic states. Similar trends were found for 2Rd as displayed in Fig. 1b.

In Fig. 2a we show the many-electron overlap factors, Eqs. (4) and (5), for electronic transitions between the neutral ground state of 3R and electronic states of the charged molecule. These results indicate which spin orbitals are involved in the electron or hole transfer process. The vertical gray line at $N = 150$ designates the highest occupied spin orbital of the neutral species. For the neutral to cation transitions (blue),[1] electrons are deleted from the occupied orbitals of the neutral molecule; for neutral to anion transitions (red), electrons are injected into the unoccupied orbitals of the neutral molecule. For 3R it is found that the tunneling rates are generally dominated by a single orbital; the higher lying excited states of the anion ($b = 5$, 6) are the exception to this. For 2Rd the situation is quite different; the overlap factors in Fig. 2b show that many different orbitals contribute significantly to the effective tunneling rates. This is especially true for transitions into the higher lying excited states of the 2Rd anion.

In addition to the wavefunction overlaps, the contribution of a given orbital to the effective tunneling rates will depend on the extent to which the electron density of the molecular orbital overlaps with electron density of the leads. The most obvious contact geometry for 3R is at the ends of the carbon skeleton and it is expected that orbitals with greater density at the ends of the molecule are likely to have a greater impact on the conductance of the junction. Figs. 3a–d depict the spatially resolved tunneling rates for transition to the four lowest energy states of anionic 3R. Figs. 3e–h show the tunneling rates transition to the four lowest energy states of the cationic 3R. The density in each panel is dominated by a contribution from a single orbital.

Combining the orbitals for 2Rd with the many-electron overlaps leads to the effective tunneling rates shown in

[1] For interpretation of color in Figs. 2 and 5, the reader is referred to the web version of this article.

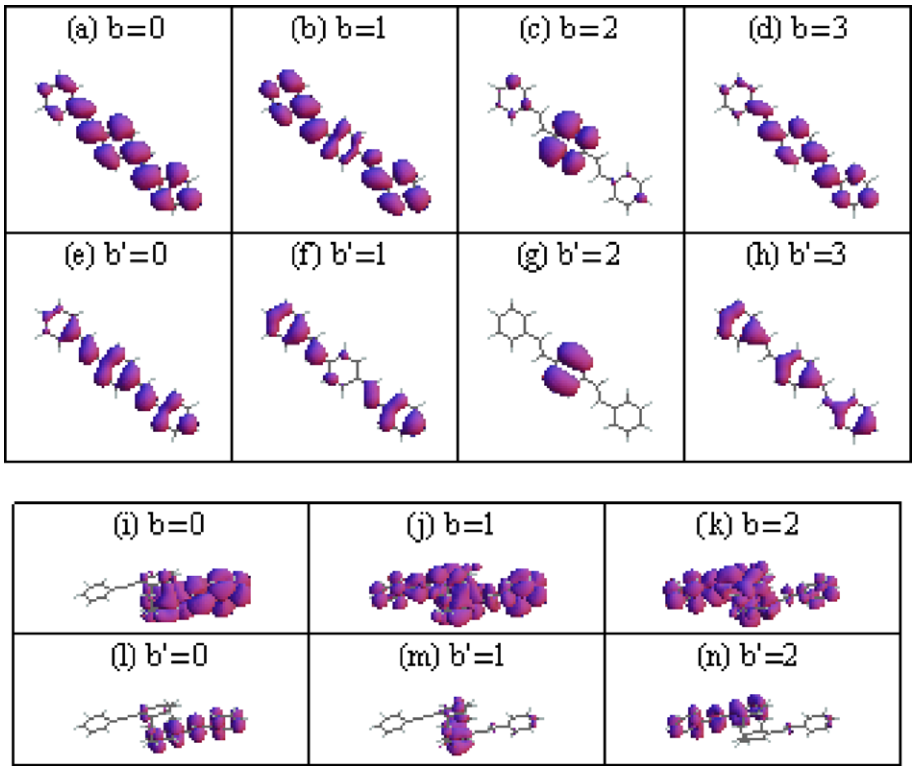

Fig. 3. Spatially resolved tunneling rates for charge transitions of (a)–(h) 3R and (i)–(n) 2Rd.

Figs. 3i–n. We note that the spatially resolved tunneling rates are very different compared to individual orbitals. The orbitals (not shown) are more or less symmetric between the upper and lower stilbene decks of the 2Rd molecule; however, the tunneling rates are very asymmetric and there is significant cancellation of intensity on one or the other side of the molecule for any given electronic transition. In panel i we see that the rate for the transition between the neutral ground state and $b = 0$ is most intense on the lower stilbene deck; for $b = 2$ the intensity is larger on the upper deck. Similar effects are seen for transitions into the cation states of 2Rd; these are shown in panels l–n, respectively.

In Figs. 4a and b we show the absolute magnitude of the CIF signal, Eq. (6), vs. $\hbar\omega_S$ and eV for 3R and 2Rd, respectively. The calculation includes the two lowest energy anio-

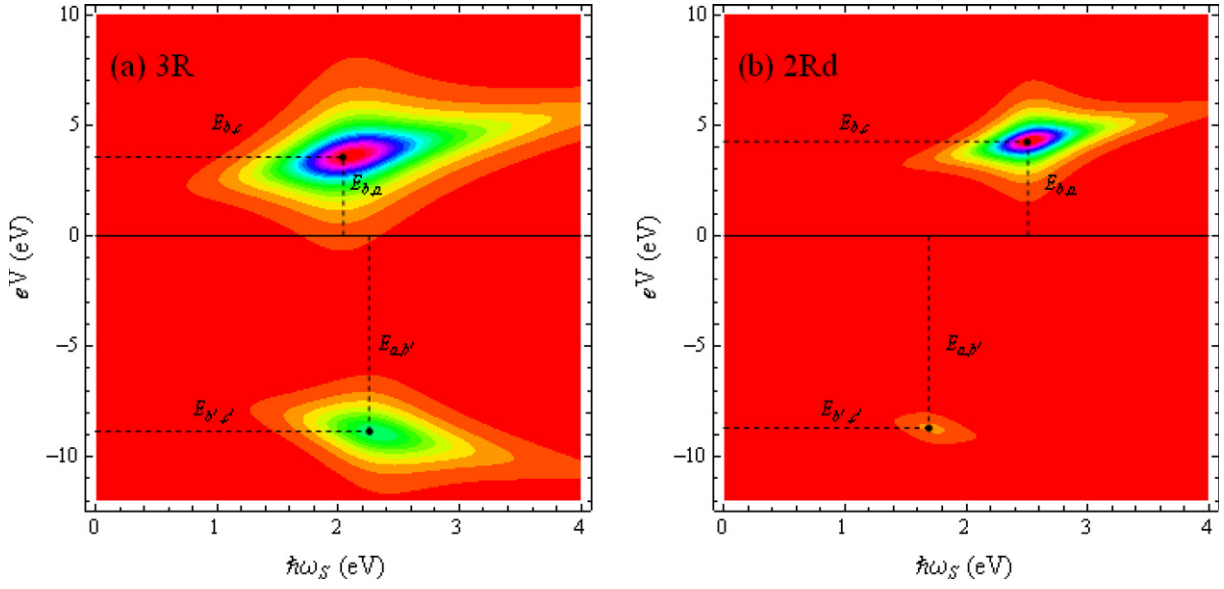

Fig. 4. CIF of (a) 3R and (b) 2Rd as a function of $\hbar\omega_S$ and eV.

nic and two lowest energy cationic states. We have neglected the spatial dependence of the tunneling rates and simply used the total of the many-electron overlaps to determine the tunneling rates. The voltage division factor for this calculation is $\eta = 1$ so that the peak at positive bias is due to emission from the first excited state of the anion to the ground anionic state; the peak at negative bias originates from the electronic transition from the first excited cationic state to the ground cationic state. Along the voltage axes, the CIF is most intense when the chemical potential is resonant with the energy difference between the excited charge state and the neutral ground state. The dashed lines indicate the energies involved in determining the positions of the peaks.

It was shown in Fig. 3b that the tunneling rates can be stronger at different places on the same molecule for transitions to either the anionic or cationic charge states. This suggests that it should be possible to control at what bias electron/hole injection becomes most favorable. One way to control the conductance properties is to manipulate the potential drop across the junction. To demonstrate this point we consider an idealized junction where the molecular bridge is reduced to a single point with a negligible charge distribution. For simplicity we consider only the neutral, anionic, and cationic ground states, respectively, a, b, and b'. The potential drops linearly across the junction and the conductance characteristics are determined by the position of the molecule between the contacts; the molecule's position is accounted for by the voltage division factor η [19].

In Fig. 5a we plot the conductance as a function of bias energy and η for this model system. The conductance peaks when either μ_L or μ_R are resonant with the frequencies $E_{ba} = 1$ eV and $E_{b'a} = 2$eV; we take $W_{ab} = W_{ab'} = 1$. The solid red and solid blue curves show the trace of the center of the peaks for resonance ($E_{ab'}$ and E_{ba}, respectively) with μ_L. The dashed red and dashed blue lines track the center of the peaks for resonance with μ_R.

In panels b–d we show the conductance as a function of bias for several values of η. Each panel contains five curves: (solid blue) the conductance from the anion at the left contact, (solid red) conductance from the cation at the left contact, (dashed blue) conductance from the anion at the right contact, (dashed red) conductance from the cation at the right contact, (solid purple) the total conductance. For $\eta = 0.5$ (panel c) the molecule is equally spaced to between the leads and so the voltage drop is completely symmetric. Both the cation and anion states give rise to peaks at positive and negative bias polarity, though the peaks are shifted and broadened by a factor of 2. For the intermediate values

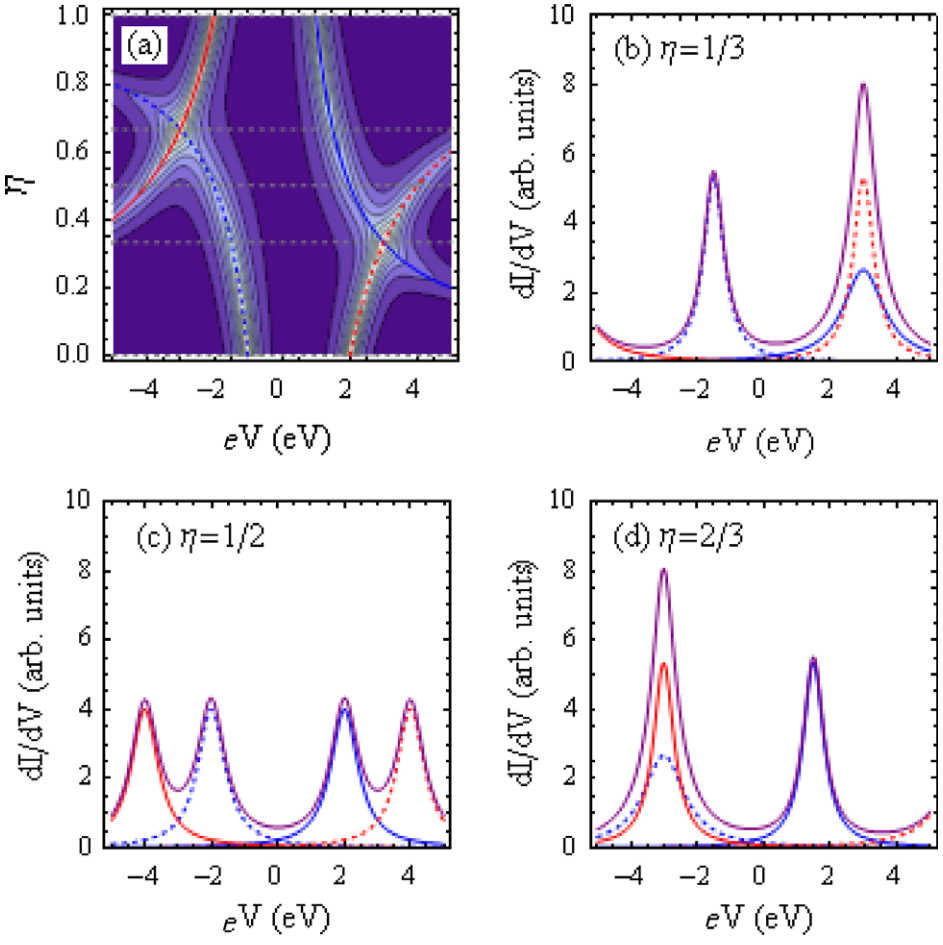

Fig. 5. (a) Conductance spectra as a function of eV and η for a model system. (b)–(d) Conductance spectra vs. eV for several η values.

of η shown in panels b and d, $\eta = 1/3$ and $\eta = 2/3$, respectively, the conductance peaks due cation and anion states overlap with either μ_L or μ_R at the same bias value. This means that electrons and holes will be injected with at the opposite sides of the junction. This situation is favorable for the creation of an exciton which may later decay releasing a photon and leaving the molecular bridge in its neutral ground state.

In order to control this process it is necessary to manipulate the contact geometry of the molecule and also the transition frequencies between the molecular charge states. Typically thiol groups are used to facilitate the chemisorption of organic molecules to gold contacts. By adding methylene spacer units with different number of carbon atoms between the thiol group and aromatic skeleton one could affect the coupling between the electronic states and the metallic leads. Additional alkane groups on the ends of the molecule will have some impact on the transition energies of the molecule. However, a more dramatic tuning of the electronic states could be realized through chemical modification of the bridge group by placing electron donating or electron withdrawing substituents at different positions on the aromatic backbone.

4. Summary

We have calculated the dI/dV and CIF spectra of single molecules in a tunneling junction in terms of both cationic and anionic electronic states. Peaks in the dI/dV are found when μ_X is resonant with the neutral-charged electronic transition energies. The spectral characteristics of the CIF reflect the energy needed to inject and electron or hole into the molecule in an excited charged state and also the electronic transition energy of the charged molecule. We suggest that the conductance and electroluminescent properties of the junction could be controlled through chemical modification of the molecular bridge; methylene spacers could potentially be employed to control the voltage drop across the molecular junction thereby changing the conductance. Electrophilic substituents could be used to adjust the relative transition frequencies between different charge states and would provide an addition dimension of control.

Acknowledgements

We gratefully acknowledge the support of the National Science Foundation NIRT (EEC-0406750), (CHE-0446555), and CBC (CHE-0533162).

References

[1] J.H. Burroughes et al., Nature 347 (1990) 539.
[2] G.C. Bazan, W.J. Oldham, R.J. Lachicotte, S. Tretiak, V. Chernyak, S. Mukamel, J. Am. Chem. Soc. 120 (1998) 9188.
[3] G.P. Bartholomew, G.C. Bazan, Acc. Chem. Res. 34 (2001) 30.
[4] G.P. Bartholomew, G.C. Bazan, J. Am. Chem. Soc. 124 (2002) 6183.
[5] G.P. Bartholomew, I. Ledoux, S. Mukamel, G.C. Bazan, J. Zyss, J. Am. Chem. Soc. 124 (2002) 13480.
[6] J.W. Hong, H.Y. Woo, B. Liu, G.C. Bazan, J. Am. Chem. Soc. 127 (2005) 7435.
[7] J.W. Hong, B.S. Gaylord, G.C. Bazan, J. Am. Chem. Soc. 124 (2002) 11868.
[8] A. Ruseckas, E.B. Namdas, J.Y. Lee, S. Mukamel, S. Wang, G.C. Bazan, V. Sunström, J. Phys. Chem. A 107 (2003) 8029.
[9] W. Leng, J. Grunden, G.P. Bartholomew, G.C. Bazan, A.M. Kelley, J. Phys. Chem. A 108 (2004) 10050.
[10] A.M. Moran, J. Chem. Phys. 124 (2006) 194904.
[11] C. Silien, N. Liu, W. Ho, J.B. Maddox, S. Mukamel, B. Liu, G.C. Bazan, Nano Lett. submitted for publication.
[12] D.S. Seferos, S.A. Trammell, G.C. Bazan, J.G. Kushmerick, Proc. Natl. Acad. Sci. USA 102 (2005) 8821.
[13] D.S. Seferos, A.S. Blum, J.G. Kushmerick, G.C. Bazan, J. Am. Chem. Soc. 128 (2006) 11280.
[14] C. Caroli, R. Combescot, P. Nozieres, D. Saint-James, J. Phys. C: Solid St. Phys. 4 (1971) 916.
[15] S. Datta, Quantum Transport: Atom to Transistor, Cambridge University Press, New York, 2005.
[16] B. Muralidharan, A.W. Ghosh, S. Datta, Phys. Rev. B 73 (2006) 155410.
[17] U. Harbola, J.B. Maddox, S. Mukamel, Phys. Rev. B 73 (2006) 205404.
[18] U. Harbola, J.B. Maddox, S. Mukamel, Phys. Rev. B 73 (2006) 075211.
[19] S. Datta, W. Tian, S. Hong, R. Reifenberger, J.I. Henderson, C.P. Kubiak, Phys. Rev. Lett. 79 (1997) 2530.
[20] Y. Xue, S. Datta, M.A. Ratner, Chem. Phys. 281 (2002) 151.
[21] J. Tersoff, D.R. Hamann, Phys. Rev. Lett. 50 (1983) 1998.
[22] J. Bardeen, Phys. Rev. Lett. 6 (1961) 57.
[23] R.J. Cave, M.D. Newton, Chem. Phys. Lett. 249 (1996) 15.
[24] P. Jaschinsky, P. Coenen, G. Pirug, B. Voightländer, Rev. Sci. Instrum. 77 (2006) 093701.
[25] A. Szabo, N.S. Ostlund, Modern Quantum Chemistry, Introduction to Advanced Electronic Structure Theory, McGraw-Hill, New York, 1989.
[26] J.B. Foresman, M. Head-Gordon, J.A. Pople, M.J. Frisch, J. Phys. Chem. 96 (1992) 135.
[27] L. Campbell, S. Mukamel, J. Chem. Phys. 121 (2004) 12323.
[28] J.B. Maddox, U. Harbola, K. Mayoral, S. Mukamel, J. Phys. Chem. C 111 (2007) 9516.
[29] S. Mukamel, Principles of Nonlinear Optical Spectroscopy, Oxford University Press, 1995.
[30] A. Nitzan, Ann. Rev. Phys. Chem. 52 (2001) 681.
[31] M. Galperin, M.A. Ratner, A. Nitzan, J. Phys.: Condens. Matter 19 (2007) 103201.
[32] M.J. Frisch et al., GAUSSIAN 03, Revision C.02, Gaussian, Inc., Wallingford, CT, 2004.